Broadband optical response of graphene measured by terahertz time-domain spectroscopy and FTIR spectroscopy

Karsten Arts[1], René Vervuurt[1], Arkabrata Bhattacharya[2,3], Jaime Gómez Rivas[1,2], Johan Willem Oosterbeek[4], Ageeth Bol[1]

[1]*Department of Applied Physics, Eindhoven University of Technology, P.O. Box 513, 5600 MB Eindhoven, The Netherlands*

[2]*Dutch Institute for Fundamental Energy Research (DIFFER), P.O. Box 6336, 5600 HH Eindhoven, The Netherlands*

[3]*Currently at Tata Institute of Fundamental Research, Mumbai 400005, India*

[4]*Euratom Association, Max-Planck-Institut für Plasmaphysik, Wendelsteinstr. 1, 17491 Greifswald, Germany*

This work describes the broadband optical response of graphene grown by Chemical Vapor Deposition (CVD) by combining terahertz Time-Domain Spectroscopy (THz-TDS) at 0.25-1.7 THz (8-60 cm^{-1}) with Fourier Transform Infrared Spectroscopy (FTIR) at 11-210 THz (370-7000 cm^{-1}). It is shown that the measured response is well described by a combination of the Drude model, expressing free-carrier absorption/reflection, and an expression for interband absorption. The THz-TDS and FTIR transmittance curves are fitted consistently using this model. This indicates that these techniques are complementary to each other. Both can thus be employed together or individually to characterize the electronic properties of graphene (e.g. carrier density and mobility). To exemplify this we demonstrate that this equivalency can be used to study the effect of substrate-dependent doping on the optical response of graphene. Furthermore, the amount of reflection and absorption corresponding to the measured transmittance curve is calculated. The toolbox for the non-invasive broadband characterization of graphene is thus extended by this work.

This manuscript was accepted by J. Appl. Phys. Click here to see the version of record.

1. Introduction

Graphene, a free-standing single atomic layer of graphite, was first isolated in 2004[1]. Since its discovery, research on graphene has grown exponentially[2] as it possesses a number of unique properties. For instance, graphene combines a very high electrical and thermal conductivity, mechanical strength and transmittance for visible light (97.7%).[3,4] Graphene's exceptional charge carrier mobility[5] makes it conductive at low carrier densities, thereby avoiding free-carrier absorption of visible and even infrared (IR) light.[6] This is essential for optoelectronic devices such as light-emitting diodes, displays and touch screens where both a high conductivity and transparency are required.[7] For example, graphene can act as a conductive electrode that is transparent for visible as well as IR light, thereby enhancing the efficiency of (IR converting[8]) solar cells.[7,9] Furthermore, graphene has recently received attention as a microwave-blocking and IR/visible/UV-transmitting coating, which are required at the diagnostic windows in nuclear fusion reactors.[10]

The optoelectronic capabilities of graphene have been explored through experimental research regarding its transmittance in the microwave[11–13], terahertz (THz)[6,12,14–16], infrared[6,17,18], visible[6,7,18–20] and ultraviolet (UV)[7,18] range of the spectrum. However, experimental data fully describing transmission, reflection and absorption for this entire range (i.e. microwave up to UV radiation) is scarcely available.

This work demonstrates that the broadband optical response of graphene is well characterized by a combination of THz Time-Domain Spectroscopy (THz-TDS)[21,22] and Fourier Transform Infrared Spectroscopy (FTIR)[23]. These diagnostics are applied to measure the transmittance of large-area CVD-grown graphene in the THz (0.25-1.7 THz or 8-60 cm^{-1}) and IR regime (11-210 THz or 370-7000 cm^{-1}). It is shown that the measured optical response is accurately described by the Drude

This manuscript was accepted by J. Appl. Phys. Click here to see the version of record.

model combined with an expression for interband absorption. This model is used to fit and extrapolate the transmittance data and to determine the electronic properties (i.e. carrier density and mobility) of graphene. It is also demonstrated how this method can be employed to determine the effect of (substrate-dependent) doping on the optical response of graphene. Finally, the reflected and absorbed fraction of power corresponding to the measured transmittance is calculated.

2. Experimental methods

Figure 1 provides a schematic description of the general experimental procedure carried out in this work. As mentioned in the introduction and described in Figure 1, the optical measurements are performed on large-area graphene (i.e. ~1 cm^2) grown by Chemical Vapor Deposition (CVD). Following the standard process reported by Vervuurt et al.[24] methane gas is used as the precursor for graphene growth on copper foil. Using spin-coated PMMA the graphene is afterwards transferred to the desired substrate. Although samples with different substrates will be discussed in Figure 4, silicon is used as the default substrate (>20 kΩcm, 510-540 µm thick, double sided polished) which has a ~50% transparency for THz and IR radiation. This transparency is high enough to reliably measure the substrate-normalized transmittance T_{sf}/T_s of the graphene by THz-TDS[21,22] and FTIR[23]. Here T_{sf} is the transmittance of the substrate and film (i.e. silicon and graphene) and T_s is the transmittance of the substrate only. Afterwards, the substrate-normalized transmittance is fitted using an optical model in which the optical conductivity of the graphene is described by the Drude model combined with an expression for interband absorption.

Figure 1: Schematic description of the adopted experimental procedure. First, graphene is grown by CVD on copper foil, after which the graphene is transferred to the desired substrate using spin-coated PMMA.[24] Next, the transmittance of THz and IR

This manuscript was accepted by J. Appl. Phys. Click here to see the version of record.

radiation is measured through a reference substrate and through the sample using THz-TDS[21,22] and FTIR[23], respectively. Finally, the transmittance of the sample is normalized by the transmittance of the substrate and analyzed using an optical model.

3. Results and discussion

A typical substrate-normalized THz-TDS and FTIR transmittance measurement is presented in Figure 2 for CVD-grown graphene on silicon. A high transmittance is measured for IR radiation, while the transmittance is strongly reduced in the THz regime due to free-carrier absorption and reflection. In the near infrared (i.e. at wavelengths below ~3 µm) the transmittance is reduced by interband absorption: electron excitation from the valence band into the conduction band. This response is comparable to results found in literature for similar large-area graphene.[6,14–17] Moreover, measurements of different samples, which are presented in Figure 4, indicate that this response is well reproducible.

Figure 2: Typical substrate-normalized transmittance T_{sf}/T_s measured by THz-TDS and FTIR for CVD-grown graphene on a silicon substrate. The THz-TDS and FTIR data are fitted consistently using a single parametrization for the optical conductivity, consisting of a Drude response and interband term as given by equations (2) and (4).

The two mechanisms governing the measured and modelled optical response, namely free-carrier conduction and interband excitation, are described by the complex frequency-dependent optical conductivity of graphene. A higher (two-dimensional) optical conductivity increases the amount absorption and/or reflection. This can be seen from the commonly used thin film approximation for the substrate-normalized transmittance:[17]

$$\frac{T_{sf}}{Ts} \approx 1 - \frac{2}{1+N_s} Z_0 \Re(\sigma_{2D}), \qquad (1)$$

where N_s is the refractive index of the substrate, $Z_0 = 1/(\epsilon_0 c) \approx 377\ \Omega$ is the vacuum impedance and σ_{2D} is the two-dimensional conductivity of the film (i.e. bulk conductivity × film thickness).

This manuscript was accepted by J. Appl. Phys. Click here to see the version of record.

By using an expression for graphene's optical conductivity the measured substrate-normalized transmittance is fitted. This expression consists of two terms: σ_{2D}^{intra} and σ_{2D}^{inter}. The first term describes the free-carrier conduction, or specifically intraband conduction (i.e. conduction through electron transitions within the same energy band). Intraband conduction can be parametrized by adopting the Drude model in which a phenomenological scattering rate Γ (rad/s) describes the amount of resistive scattering of the electrons or holes:[25,26]

$$\sigma_{2D}^{intra} = \frac{ie^2 2k_B T}{\pi\hbar^2(\omega+i\Gamma)} \ln[2\cosh(\mu_c/2k_B T)], \quad (2)$$

which approaches

$$\sigma_{2D}^{intra} = \frac{ie^2}{\pi\hbar^2}\frac{\mu_c}{\omega+i\Gamma} \quad (3)$$

for $\mu_c \gg k_B T$. Here ω is the angular frequency of the electromagnetic wave, e is the elementary charge, $\hbar = h/2\pi$ is the reduced Planck's constant, k_B is the Boltzmann's constant, T is the temperature and μ_c is the chemical potential. The chemical potential is set by the carrier density $n_{2D} = (\mu_c/\hbar v_F)^2/\pi$,[25] and Fermi velocity $v_F = 10^6$ m/s.[27–29]

A second term, describing interband conductivity, is added to describe the optical conductivity for the whole spectral range measured. Interband conduction takes place when the energy $\hbar\omega$ of the incident photon is high enough to overcome Pauli blocking and excite electrons from the lower into the upper Dirac cone. This typically applies for near infrared and shorter wavelength radiation, when $\hbar\omega \geq 2\mu_c$.[18] In this work the interband conductivity is approximated by[25]

$$\sigma_{2D}^{inter} = \frac{e^2}{4\hbar}\left(\frac{1}{2} + \frac{1}{\pi}\arctan\left[\frac{\hbar\omega-2\mu_c}{2k_B T}\right] - \frac{i}{2\pi}\ln\left[\frac{(\hbar\omega+2\mu_c)^2}{(\hbar\omega-2\mu_c)^2+(2k_B T)^2}\right]\right), \quad (4)$$

which approaches the universal value of $\sigma_0 = e^2/4\hbar$ for $\hbar\omega \gg 2\mu_c$.

This manuscript was accepted by J. Appl. Phys. Click here to see the version of record.

The fit through the data plotted in Figure 2 is thus obtained by inserting equations (2) and (4) in an optical model. Instead of using equation (1) for this purpose, more accurate equations reported by Maley[30] are used. This optical model assumes a thin film with coherent multiple reflections on a finite substrate with incoherent multiple reflections. Moreover, a constant refractive index $N_s = 3.42$ of the silicon substrate is assumed[31] and the temperature in equations (2) and (4) is set to 300 K. Aside from the chemical potential and scattering rate, a small conductivity σ_{2D}^{offset} (<20 µS) is fitted as well. This parameter accounts for IR absorption by the PMMA residue left on the graphene as a result of the transfer process to the final substrate.[32] After fitting the substrate-normalized transmittance, the same optical model is used to calculate the transmittance T_f, reflectance R_f and absorption A_f of the graphene only, where the substrate is excluded by setting $N_s = 1$ in the calculation.

According to the fit, the graphene measured in Figure 2 has a scattering rate of $\Gamma = 17$ rad/s $= 2.7$ THz and a chemical potential of $\mu_c = 0.31$ eV. This corresponds to a carrier density $n_{2D} = 6.9 \times 10^{12}$ cm^{-2}, mobility $\mu = 2.0 \times 10^3$ cm^{2}Vs and sheet resistance $R_s = 4.6 \times 10^2$ Ω/□ (read: Ohm per square). These values compare well to those reported in literature for CVD-grown graphene.[17,33–38] As an illustrative example of graphene's optical conductivity, the real and imaginary part of the fitted $\sigma_{2D} = \sigma_{2D}^{intra} + \sigma_{2D}^{inter}$ are plotted against frequency in Figure 3.

Figure 3: Real and imaginary part of the 2D optical conductivity $\sigma_{2D}^{intra} + \sigma_{2D}^{inter}$ of graphene for $\Gamma = 17$ rad/s $= 2.7$ THz and $\mu_c = 0.31$ eV as fitted in Figure 2. Interband excitation takes place for near IR, visible and UV radiation when $\hbar\omega \geq 2\mu_c$ as described by equation (4), while intraband conduction (equation (2)) is dominant at sub-THz frequencies where $\omega \leq \Gamma$.

The curve fitted in Figure 2 shows a good correspondence with the THz-TDS data and with the FTIR data as well. This suggests that the optical response of graphene can be described for the entire plotted spectral range by a simple Drude response and interband excitation term. Regarding

the interband term, the calculated 2.3% interband absorption indeed agrees with measurements done by Nair et al. using white light.[19] However, equation (4) does not accurately describe interband excitation for wavelengths below ~500 nm. Here a higher absorption is measured in literature, reaching roughly 9% at 270 nm.[7,18–20] This is because a constant interband absorption is only found in the linear dispersion regime of graphene where the optical conductivity has the universal value of $\sigma_0 = e^2/4\hbar$. For energies above ~2 eV, the Dirac cone approximation is no longer valid and an absorption peak around 4.5 eV (or 270 nm) should be included.[18,39,40]

The good correspondence between the THz-TDS and FTIR data also demonstrates that THz-TDS and FTIR transmittance measurements of CVD-grown graphene are complementary to each other. Both can be fitted independently following the described approach, typically yielding the same electronic properties (e.g. carrier density and mobility) within a deviation of a few percent. Here care should be taken when fitting FTIR data of CVD-grown graphene, since IR absorption by (PMMA) residue can significantly alter the fit if not properly accounted for. The indicated equivalency of THz-TDS and FTIR measurements of graphene is particularly useful for cases where the used substrate is only suitable for one of the techniques. For example, the substrate can be opaque or have a large variation in its refractive index in one of the spectral ranges.

An example is now presented on how the shown THz-TDS/FTIR equivalency can be exploited. Here, the THz-TDS/FTIR measurement and fitting procedure is carried out for CVD-grown graphene transferred to three different substrates: quartz (1 sample), silicon (3 samples) and silicon treated with an O_2 plasma (3 samples). Since quartz is not transparent for IR radiation, only the THz-TDS spectrum is measured and fitted for this sample, which predicts the IR response of the graphene as well. From the measured and fitted substrate-normalized transmittance T_{sf}/T_s, given in panel (A) of Figure 4, the transmittance T_f of the graphene is calculated to exclude the

contribution of the substrate. The resulting T_f-curves are plotted in panel (B) of Figure 4. Most notably, Figure 4 shows that the cutoff frequency, below which radiation is blocked by intraband conduction, is dependent on the used substrate. Here the cutoff frequency is defined as $\omega = \Gamma$, where $\Re\left(\sigma_{2D}^{intra}\right)$ is at half its maximum value as shown in Figure 3. The same shift is seen for the frequency $\omega = 2\mu_c/\hbar$ above which interband absorption takes place. These observations indicate that the mobility and carrier density, so the doping of the graphene, is substrate-dependent.[41–43] Even though the carrier density and mobility of these samples are different due to substrate-dependent doping, their product $n\mu$ is similar such that all samples have a sheet resistance of ~500 Ω/□ and correspondingly a ~52% transmittance for wavelengths above 1 mm (i.e. for microwave radiation). The observed substrate-dependency of the doping of graphene is in agreement with electronic measurements and Raman spectroscopy carried out in literature.[41–43] This example thus demonstrates how THz-TDS and FTIR can be combined or performed individually to investigate electronic behavior of graphene in a non-invasive way.

Figure 4: Panel (A): Fitted substrate-normalized transmittance T_{sf}/T_s measured by THz-TDS and FTIR for CVD-grown graphene transferred to quartz (one sample, dotted red), silicon (three samples, solid black) and silicon treated with an O_2 plasma (three samples, dashed blue). Since quartz is not transparent for infrared radiation ($T_s = 0$) only the THz-TDS spectrum is measured and fitted for this sample. Note that the value of T_{sf}/T_s is lower when measuring on a substrate with a lower refractive index, as seen in equation 1. Panel (B): Calculated transmittance T_f of graphene corresponding to the THz-TDS/FTIR data fitted in panel (A). The measurements illustrate that the mobility and carrier density are substrate-dependent, which is reflected in a shifted cutoff frequency ($\omega = \Gamma$) and a shifted minimum energy needed for interband excitation ($\hbar\omega = 2\mu_c$).

For some applications not only the transmission of graphene but also its absorption and reflection may be of interest, for example to assess the amount of heat dissipated in the graphene. With the same equations as those used for fitting the THz-TDS/FTIR data of Figure 2, the power transmission, absorption and reflection corresponding to this fit are calculated and plotted in Figure

5. Again, these curves are computed for $N_s = 1$ to show the contribution of the graphene only. According to this calculation, the graphene (having a sheet resistance of 460 Ω/□) absorbs 41.3% and reflects 8.5% microwave power, giving circa 50% microwave transmittance as seen before in Figure 4. The transmission, reflection and absorption of microwave power calculated for graphene with $R_s = 635$ Ω/□ agree with measurements performed at 2.2-7 GHz by Hong et al. on such CVD-grown graphene.[11] This validates Figure 5 at the low frequency side of the spectrum. At the high frequency side Figure 5 shows that reflection of (near) IR, visible and UV radiation is negligible compared to the calculated 2.3% interband absorption.

Figure 5: Power transmission T_f (black, solid), absorption A_f (red, dashed) and reflection R_f (blue, dotted) of typical CVD-grown graphene, calculated using equations reported by Maley et al.[30] for $N_s = 1$ (i.e. excluding the substrate). This calculation corresponds to the fitted THz-TDS and FTIR data shown in Figure 2.

4. Conclusion

To conclude, in this work THz-TDS at 0.25-1.7 THz (8-60 cm^{-1}) and FTIR at 11-210 THz (370-7000 cm^{-1}) were combined to measure the broadband optical response of large-area CVD-grown graphene. A high transmittance (>90%) was found for (near) infrared radiation while the graphene blocks up to ~50% power in the microwave/THz regime, which is calculated to be mostly by absorption. Even while having this high IR transparency the graphene has a reasonable sheet resistance of roughly 500 Ω/□. This affirms graphene's potential for optoelectronic applications such as touch screens or solar cells, where a high transparency for IR, visible and/or UV needs to be combined with a high conductivity. Furthermore, it was demonstrated that THz-TDS and FTIR transmittance data of graphene can be fitted consistently using a simple Drude response added to an expression describing interband excitation. This makes these methods complementary to each

other, which further extends the toolbox for the non-invasive broadband characterization of graphene.

ACKNOWLEDGEMENTS

The authors would like to thank C. O. van Bommel, C. A. A. van Helvoirt, J. J. L. M. Meulendijks, and J. J. A. Zeebregts for technical assistance. N. J. J. Hoof, A. Halpin and M. Vennik are acknowledged for helping with the THz-TDS measurements. We thank the financial support of ERC through grant No. 259272 THZ-PLASMON and grant No. 665619 MicroMap. This work is part of the research program of the Foundation for Fundamental Research on Matter (FOM), which is part of The Netherlands Organization for Scientific Research (NWO).

REFERENCES

[1] K.S. Novoselov, A.K. Geim, S. V. Morozov, D. Jiang, Y. Zhang, S. V. Dubonos, I. V. Grigorieva, and A.A. Firsov, Science **306**, 666 (2004).

[2] E.P. Randviir, D.A.C. Brownson, and C.E. Banks, Mater. Today **17**, 426 (2014).

[3] K.S. Novoselov, V.I. Fal, L. Colombo, P.R. Gellert, M.G. Schwab, K. Kim, V.I.F. Ko, L. Colombo, P.R. Gellert, M.G. Schwab, and K. Kim, Nature **490**, 192 (2012).

[4] A.K. Geim, Science **324**, 1530 (2009).

[5] S. V. Morozov, K.S. Novoselov, M.I. Katsnelson, F. Schedin, D.C. Elias, J.A. Jaszczak, and A.K. Geim, Phys. Rev. Lett. **100**, 016602 (2008).

[6] J.M. Dawlaty, S. Shivaraman, J. Strait, P. George, M. Chandrashekhar, F. Rana, M.G. Spencer, D. Veksler, and Y. Chen, Appl. Phys. Lett. **93**, 131905 (2008).

[7] F. Bonaccorso, Z. Sun, T. Hasan, and A.C. Ferrari, Nat. Photonics **4**, 611 (2010).

[8] X. Huang, S. Han, W. Huang, and X. Liu, Chem. Soc. Rev. **42**, 173 (2013).

[9] C.G. Granqvist, Sol. Energy Mater. Sol. Cells **91**, 1529 (2007).

[10] R. König, J. Baldzuhn, C. Biedermann, R. Burhenn, S. Bozhenkov, A. Cardella, M. Endler, H.J. Hartfuss, D. Hathiramani, D. Hildebrandt, M. Hirsch, M. Jakubowski, G. Kocsis, P. Kornejev, M. Krychowiak, H.P. Laqua, M. Laux, J.W. Oosterbeek, E. Pasch, T. Richert, W. Schneider, T. Sunn-Pedersen, H. Thomsen, A. Weller, A. Werner, R. Wolf, D. Zhang, and S. Zoletnik, Rev. Sci. Instrum. **81**, 10E133 (2010).

[11] S.K. Hong, K.Y. Kim, T.Y. Kim, J.H. Kim, S.W. Park, J.H. Kim, and B.J. Cho, Nanotechnology **23**, 455704 (2012).

[12] N. Rouhi, S. Capdevila, D. Jain, K. Zand, Y.Y. Wang, E. Brown, L. Jofre, and P. Burke, Nano Res. **5**, 667 (2012).

[13] J.S. Gómez-Díaz, J. Perruisseau-Carrier, P. Sharma, and A. Ionescu, J. Appl. Phys. **111**, 114908 (2012).

[14] C.J. Docherty and M.B. Johnston, J. Infrared, Millimeter, Terahertz Waves **33**, 797 (2012).

[15] I.H. Baek, K.J. Ahn, B.J. Kang, S. Bae, B.H. Hong, D.I. Yeom, K. Lee, Y.U. Jeong, and F. Rotermund, Appl. Phys. Lett. **102**, 191109 (2013).

[16] H.Y. Hwang, N.C. Brandt, H. Farhat, A.L. Hsu, J. Kong, and K.A. Nelson, J. Phys. Chem. B **117**, 15819 (2013).

[17] J.W. Weber, A.A. Bol, and M.C.M. Van De Sanden, Appl. Phys. Lett. **105**, 013105 (2014).

[18] K.F. Mak, L. Ju, F. Wang, and T.F. Heinz, Solid State Commun. **152**, 1341 (2012).

[19] R.R. Nair, P. Blake, A.N. Grigorenko, K.S. Novoselov, T.J. Booth, T. Stauber, N.M.R. Peres, and A.K. Geim, Science **320**, 1308 (2008).

[20] J.W. Weber, V.E. Calado, and M.C.M. Van De Sanden, Appl. Phys. Lett. **97**, 091904 (2010).

[21] M. Tonouchi, Nat. Photonics **1**, 97 (2007).

[22] R. Ulbricht, E. Hendry, J. Shan, T.F. Heinz, and M. Bonn, Rev. Mod. Phys. **83**, 543 (2011).

[23] G. Horlick, Appl. Spectrosc. **22**, 617 (1968).

[24] R.H.J. Vervuurt, B. Karasulu, M.A. Verheijen, W.M.M. Kessels, and A.A. Bol, Chem. Mater. **29**, 2090 (2017).

[25] L.A. Falkovsky, J. Phys. Conf. Ser. **129**, 012004 (2008).

[26] G.W. Hanson, J. Appl. Phys. **103**, 064302 (2008).

[27] M. Sprinkle, D. Siegel, Y. Hu, J. Hicks, A. Tejeda, A. Taleb-Ibrahimi, P. Le Fèvre, F. Bertran, S. Vizzini, H. Enriquez, S. Chiang, P. Soukiassian, C. Berger, W.A. De Heer, A. Lanzara, and E.H. Conrad, Phys. Rev. Lett. **103**, 226803 (2009).

[28] Z.Q. Li, E.A. Henriksen, Z. Jiang, Z. Hao, M.C. Martin, P. Kim, H.L. Stormer, and D.N. Basov, Nat. Phys. **4**, 532 (2008).

[29] D.C. Elias, R. V. Gorbachev, A.S. Mayorov, S. V. Morozov, A.A. Zhukov, P. Blake, L.A. Ponomarenko, I. V. Grigorieva, K.S. Novoselov, F. Guinea, and A.K. Geim, Nat. Phys. **7**, 701 (2011).

[30] N. Maley, Phys. Rev. B **46**, 2078 (1992).

[31] Tydex J.S. Co. Silicon. Retrieved from

[31] Http//Www.Tydexoptics.Com/Materials1/For_transmission_optics/Silicon/ (2016).

[32] Y.-C. Lin, C.-C. Lu, C.-H. Yeh, C. Jin, K. Suenaga, and P.-W. Chiu, Nano Lett. **12**, 414 (2012).

[33] Z. Yan, J. Lin, Z. Peng, Z. Sun, Y. Zhu, L. Li, C. Xiang, E.L. Samuel, C. Kittrell, and J.M. Tour, ACS Nano **6**, 9110 (2012).

[34] S. Bae, H. Kim, Y. Lee, X. Xu, J.-S. Park, Y. Zheng, J. Balakrishnan, T. Lei, H. Ri Kim, Y. Il Song, Y.-J. Kim, K.S. Kim, B. Özyilmaz, J.-H. Ahn, B.H. Hong, and S. Iijima, Nat. Nanotechnol. **5**, 574 (2010).

[35] X. Li, Y. Zhu, W. Cai, M. Borysiak, B. Han, D. Chen, R.D. Piner, L. Colomba, and R.S. Ruoff, Nano Lett. **9**, 4359 (2009).

[36] X. Li, W. Cai, J. An, S. Kim, J. Nah, D. Yang, R. Piner, A. Velamakanni, I. Jung, E. Tutuc, S.K. Banerjee, L. Colombo, and R.S. Ruoff, Science **324**, 1312 (2009).

[37] K.S.K.S. Kim, Y. Zhao, H. Jang, S.Y. Lee, J.M. Kim, K.S.K.S. Kim, J.-H. Ahn, P. Kim, J.-Y. Choi, and B.H. Hong, Nature **457**, 706 (2009).

[38] S. De and J.N. Coleman, ACS Nano **4**, 2713 (2010).

[39] L. Yang, J. Deslippe, C.H. Park, M.L. Cohen, and S.G. Louie, Phys. Rev. Lett. **103**, 186802 (2009).

[40] T. Stauber, N.M.R. Peres, and A.K. Geim, Phys. Rev. B - Condens. Matter Mater. Phys. **78**, 085432 (2008).

[41] Y. Shi, X. Dong, P. Chen, J. Wang, and L.J. Li, Phys. Rev. B - Condens. Matter Mater. Phys. **79**, 115402 (2009).

[42] M. Lafkioti, B. Krauss, T. Lohmann, U. Zschieschang, H. Klauk, K. V. Klitzing, and J.H. Smet, Nano Lett. **10**, 1149 (2010).

[43] S. Ryu, L. Liu, S. Berciaud, Y.J. Yu, H. Liu, P. Kim, G.W. Flynn, and L.E. Brus, Nano Lett. **10**, 4944 (2010).

CVD of graphene and transfer to substrate (e.g. silicon or quartz)

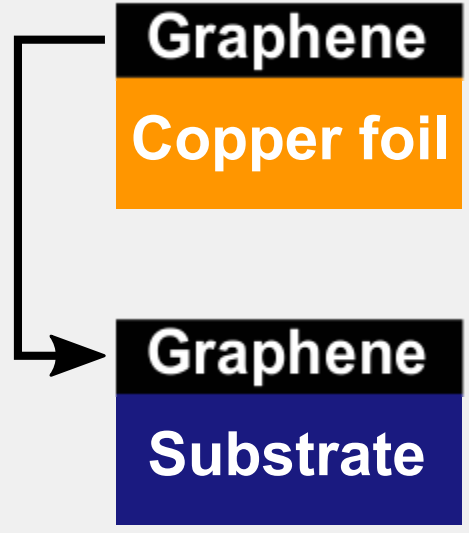

THz and IR transmittance measurements by THz-TDS and FTIR

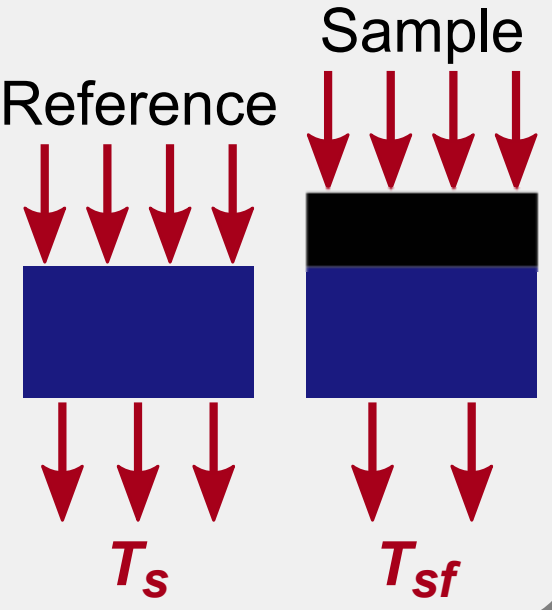

Analysis of substrate-normalized transmittance

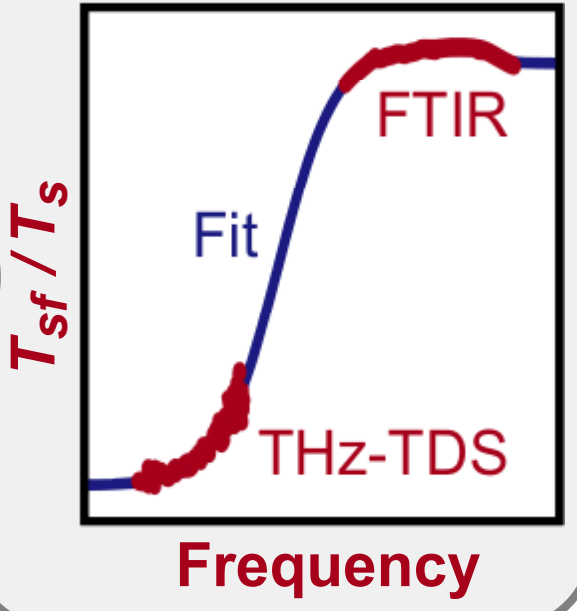

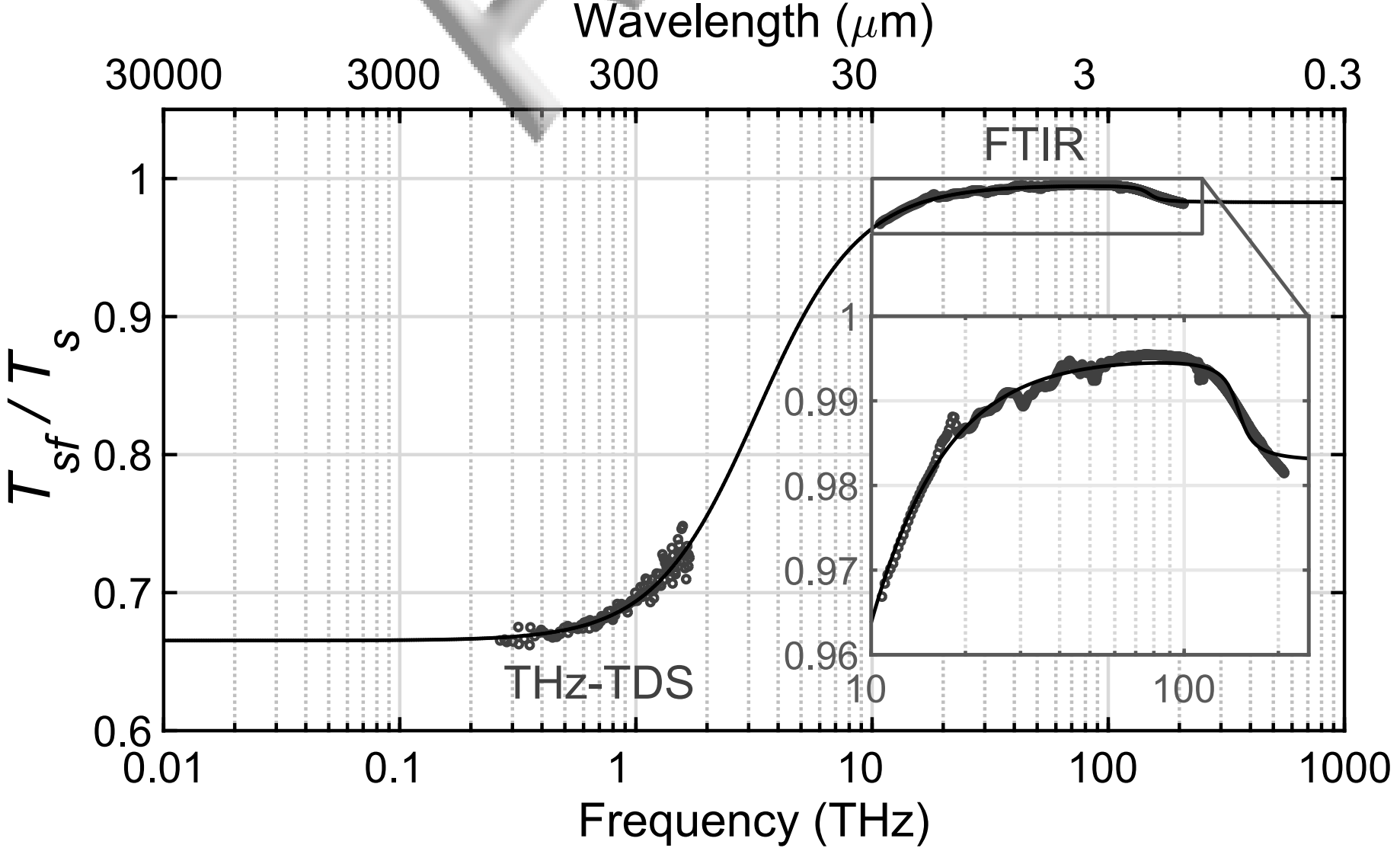
Wavelength (μm)
30000
3000
300
30
3
0.3
T_{sf} / T_s
1
0.9
0.8
0.7
0.6
0.01
0.1
1
10
100
1000
Frequency (THz)
THz-TDS
FTIR
1
0.99
0.98
0.97
0.96
10
100

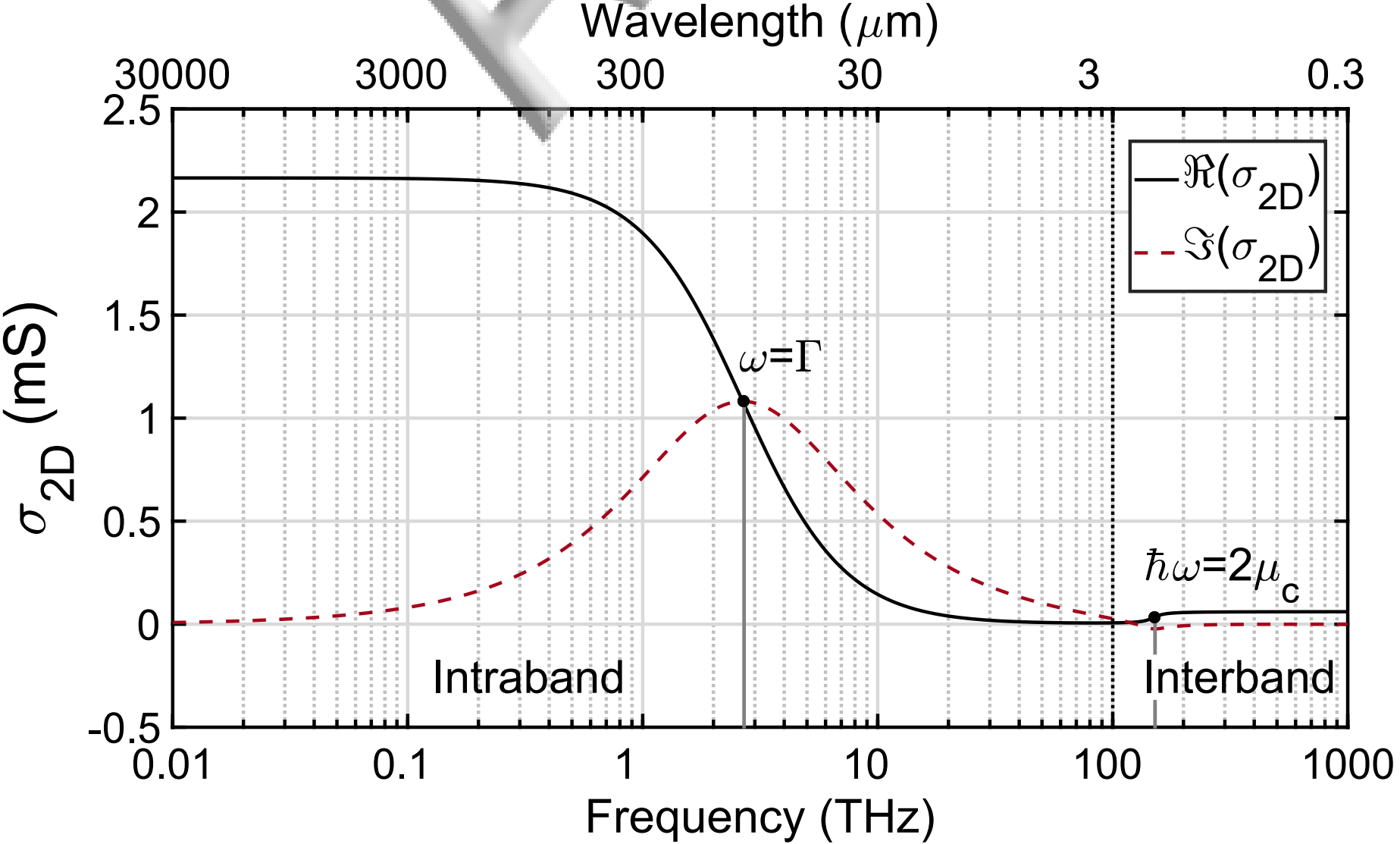
Wavelength (μm)
30000
3000
300
30
3
0.3
2.5
2
1.5
1
0.5
0
-0.5
σ_{2D} (mS)
$\Re(\sigma_{2D})$
$\Im(\sigma_{2D})$
$\omega=\Gamma$
$\hbar\omega=2\mu_c$
Intraband
Interband
0.01
0.1
1
10
100
1000
Frequency (THz)

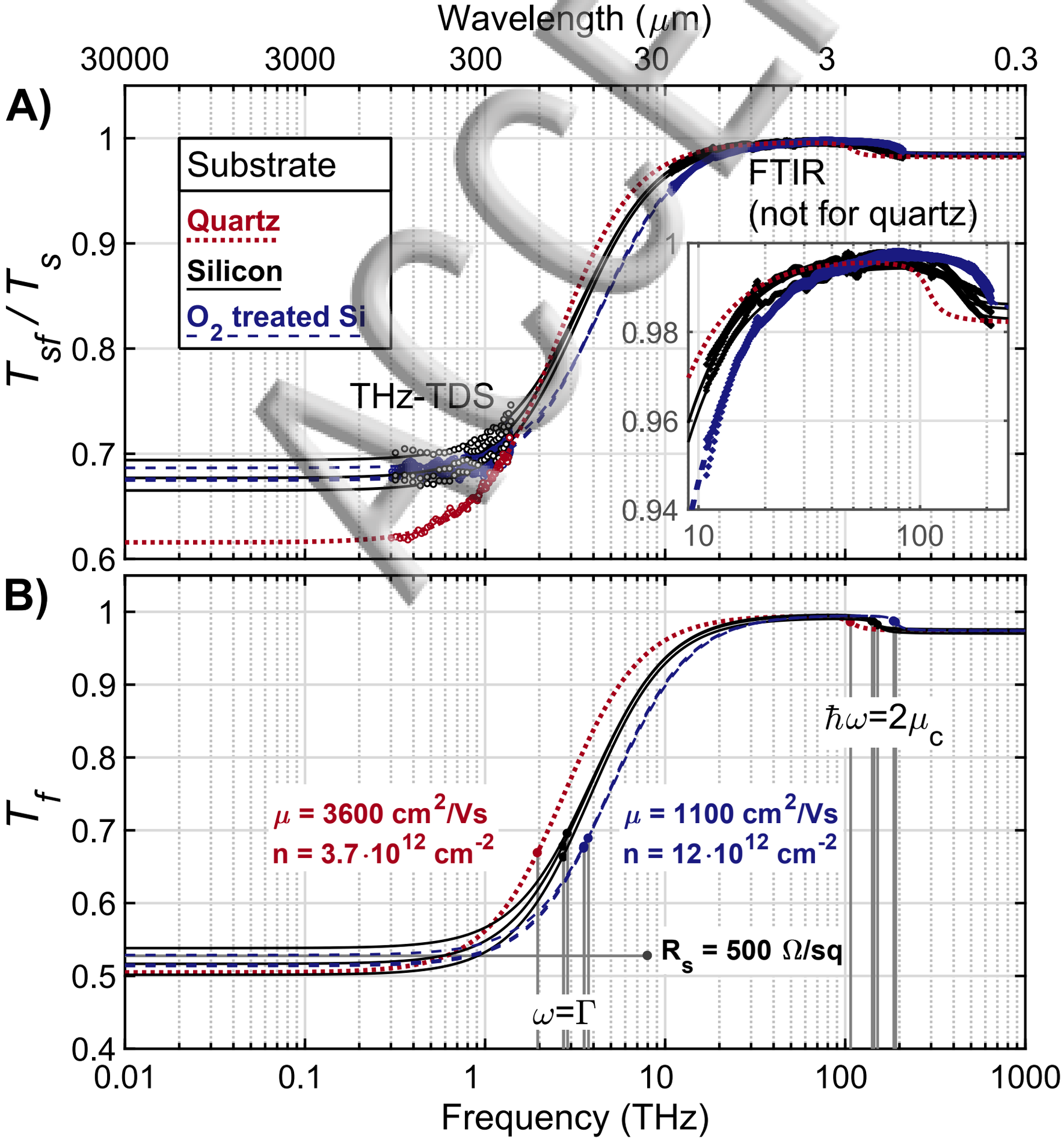
Wavelength (μm)
30000
3000
300
30
3
0.3
A)
B)
Substrate
Quartz
Silicon
O2 treated Si
THz-TDS
FTIR
(not for quartz)
T_sf / T_s
T_f
μ = 3600 cm²/Vs
n = 3.7·10¹² cm⁻²
μ = 1100 cm²/Vs
n = 12·10¹² cm⁻²
R_s = 500 Ω/sq
ħω=2μ_c
ω=Γ
Frequency (THz)
0.01
0.1
1
10
100
1000

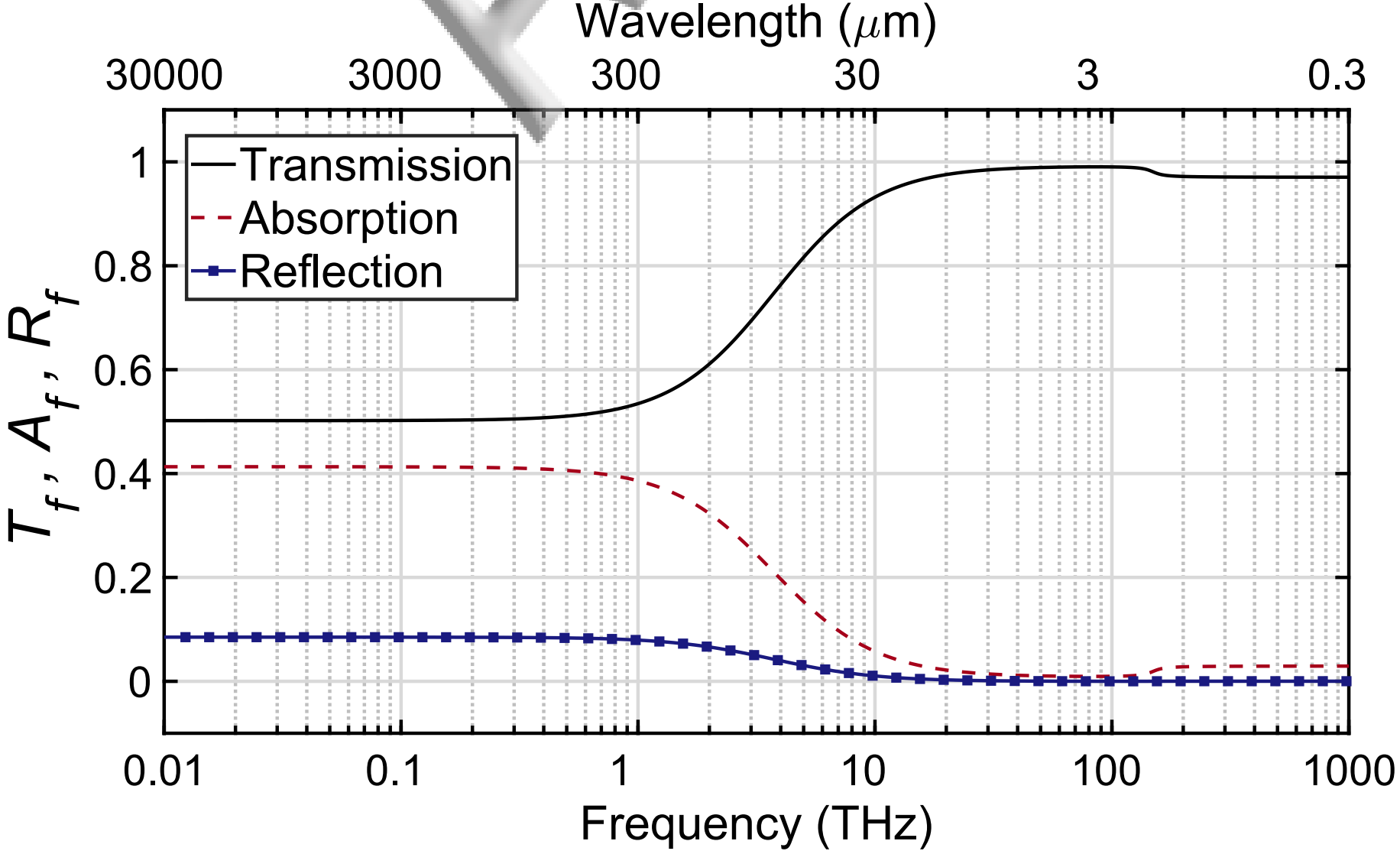
Wavelength (μm)
30000
3000
300
30
3
0.3
Transmission
Absorption
Reflection
T_f, A_f, R_f
1
0.8
0.6
0.4
0.2
0
0.01
0.1
1
10
100
1000
Frequency (THz)